TRACKING CONTROL OF A WELDING MOBILE ROBOT BASED ON AAPTIVE BACKSTEPPING METHOD

Seong Jin Ma, Tan Lam Chung, Young Bok Kim, and Myung Suck Oh

School of Mechanical Engineering, Pukyong National University, Pusan 608-739, Korea

ABSTRACT

In this paper, an adaptive controller is proposed and applied to two-wheeled welding mobile robot to track a smooth curved welding path. The mobile robot is considered in terms of dynamics model in Cartesian coordinates with unknown parameters such as moment of inertia, wheel radius and distance from the center of the platform to a rear wheel of the mobile robot. The system is considered with the nonholonomic constraints in relation with its coordinates and the reference welding path. To obtain the controller, the tracking errors are defined, and the controller is derived based on backstepping technique to guarantee that the tracking errors converge to zero asymptotically. In the proposed controller, the unknown parameters are estimated using update laws in adaptive control scheme. To obtain the tracking errors, a simple measurement scheme using touch sensor is proposed. The touch sensor consists of two potentiometers including one linear potentiometer for measuring distance error, and one rotating potentiometer for measuring angular error. To implement the experiment, a control system is developed based on the integration of three PIC18F452's: two for servo DC motor controllers, and one for main controller. The two servo controllers can perform indirect servo control using one encoder. The main controller which functions as master links to the three servo controllers, as slave, via I2C communication. Also, the simulation and experimental results are included to illustrate the performance of the proposed controller.

1. INTRODUCTION

Automatic control of welding process is widely used in many branches of industry such as building construction, pipelines, aircraft, ship fabrication, automobiles, etc. And one of the most complex applications is welding systems based on mobile robots that can give several benefits: generating a perfect welding movement and producing a consistent weld penetration and weld strength.

Mobile robot under nonholonomic constraints has been attracted much attention of many researchers in literature. Fierro, 1995, developed a combined kinematic and torque control law using backstepping approach, and the asymptotic stability is guaranteed by Lyapunov [3]. In this design, the parameters of the mobile robot are necessary, which is almost impossible to obtain exactly in practice: it is needed to be estimated. To solve this problem, some adaptive feedback controllers have been proposed to solve the tracking problem in terms of the dynamics model. T. Fukao, 2000, proposed the integration of a kinematic controller and a torque controller for the dynamic model of a nonholonomic mobile robot. In this design, a kinematics adaptive tracking controller is proposed, and then a torque adaptive controller with unknown parameters is derived using the kinematic controller [1]. T. H. Bui et al., 2003, proposed the adaptive nonlinear controller for two-wheeled welding mobile robot tracking a smooth-curved welding path using Lyapunov function candidate with the unknown parameter of moment of inertia [2]. He also proposed the adaptive nonlinear controller for two-wheeled welding mobile robot tracking a smooth-curved welding path using Lyapunov function candidate with the unknown parameter such as wheel radius and distance from the center of the platform to a rear wheel of the mobile robot [2]. However, he considered two adaptive controllers to be separated. He also consider fixed torch and controllable torch. In the fixed torch, all tracking errors goes to zero very slowly as time goes to infinity. To solve this problem, he considered the controllable torch. In this case, one control system is needed to control the torch.

This paper proposed a modified controller of the kinematic controller reported by Bui and the adaptive

controller for two-wheeled welding mobile robot to track a smooth-curved welding path even in the model of the dynamical system containing constant unknown parameters such as such as moment of inertia, wheel radius and distance from the center of the platform to a rear wheel of the mobile robot. These controllers are derived based on backstepping technique. The stability is proven using the Lyapunov method. To design the tracking controller, the errors are defined between the welding point on torch and the reference point moving at a specified constant speed on welding path. To realize the above controllers, a simple way for sensing the tracking errors using potentiometers is introduced. To implement the experiment, a control system is developed based on the integration of three PIC18F452's: two for servo DC motor controllers, and one for main controller. The two servo controllers can perform indirect servo control using one encoder. The main controller which functions as master links to the three servo controllers, as slave, via I2C communication. Additionally, the simulation and experimental results have been done to show the effectiveness of the proposed controller.

2. DYNAMIC MODEL OF WMR

In this section, the dynamic of two-wheeled welding mobile robot is considered with the nonholonomic constraints in relation with its coordinates and the reference welding path.

It is observable that the welding point is away from the WMR's center; consequently, this makes tracking error which is perpendicular to the mobile robot motion slow to converge. Therefore, the welding mobile robot used in this paper is of two-wheel mobile robot with some modifications on mechanical structure for welding application (Fig. 1). Therefore, the welding mobile robot was designed to have two motions of left and right driving wheels with fixed torch in this paper.

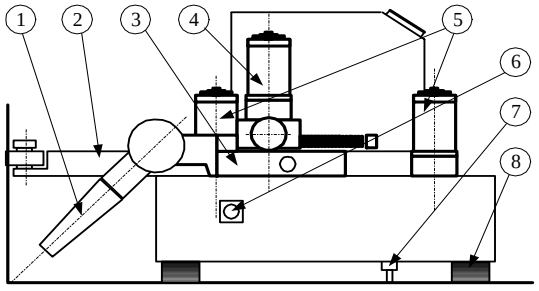

1 *welding torch*
2 *sensor*
3 *torch slider*
4 *torch slider deiving motor*
5 *wheels driving motors*
6 *proximity sensor*
7 *lower limit switch*
8 *driving wheels*

Fig. 1 WMR configuration

The model of two-wheeled welding mobile robot is shown in Fig. 2. The posture of the mobile robot can be described by three generalized coordinates:

$$q = \begin{bmatrix} x & y & \phi \end{bmatrix}^T \tag{1}$$

where, (x, y) is Cartesian coordinates of the WMR's center and ϕ is the heading angle of the WMR

Also it is chosen the internal state variables as follows

$$z = \begin{bmatrix} v & \omega \end{bmatrix}^T \tag{2}$$

It is assumed that the wheels roll and do not slip, that is, the robot can only move in the direction normal to the axis of the driving wheels. Analytically, the mobile base satisfies the conditions as the following

$$\dot{y}\cos\phi - \dot{x}\sin\phi = 0 \tag{3}$$

The dynamic model for the above wheeled mobile robot is given as follows [8]

$$\begin{cases} \ddot{x} = \dfrac{\lambda}{m}\sin\phi + b_1 u_1 \cos\phi \\ \ddot{y} = -\dfrac{\lambda}{m}\cos\phi + b_1 u_1 \cos\phi \\ \ddot{\phi} = b_2 u_2 \end{cases} \tag{4}$$

where $b_1 = 1/(rm)$, $b_2 = b/(rI)$, and that m and I denote the mass and the moment of inertia of the mobile robot, respectively. Also, $u_1 = T_1 + T_2$ and $u_2 = T_1 - T_2$ are the control inputs, and λ is the Lagrange multiplier, given by $\lambda = -m\dot{\phi}(\dot{x}\cos\phi + \dot{y}\sin\phi)$. The assumption that the signs of b_1 and b_2 are known is practical since b_1 and b_2 represent combinations of the robot's mass, moment of inertia, wheel radius, and distance between the rear wheels constant with known signs.

First, the kinematic equations of the WMR in the Cartesian space corresponding to are set up as the following

$$\begin{bmatrix} \dot{x} \\ \dot{y} \\ \dot{\phi} \end{bmatrix} = \begin{bmatrix} \cos\phi & 0 \\ \sin\phi & 0 \\ 0 & 1 \end{bmatrix} \begin{bmatrix} v \\ \omega \end{bmatrix} \tag{5}$$

The relationship between ω and the angular velocities of two driving wheels is the following

$$\begin{bmatrix} \omega_{rw} \\ \omega_{lw} \end{bmatrix} = \begin{bmatrix} 1/r & b/r \\ 1/r & -b/r \end{bmatrix} \begin{bmatrix} v \\ \omega \end{bmatrix} \tag{6}$$

where ω_{rw}, ω_{lw} represent the angular velocities of right and left wheels, b is distance from WMR's center point to the driving wheel, r is the radius of wheel.

Second, the welding point $W(x_w, y_w)$ on torch and its orientation angle ϕ_w can be derived from WMR's center $C(x, y)$ as

$$\begin{cases} x_w = x - l\sin\phi \\ y_w = y + l\cos\phi \\ \phi_w = \phi \end{cases} \tag{7}$$

where l is the length of torch

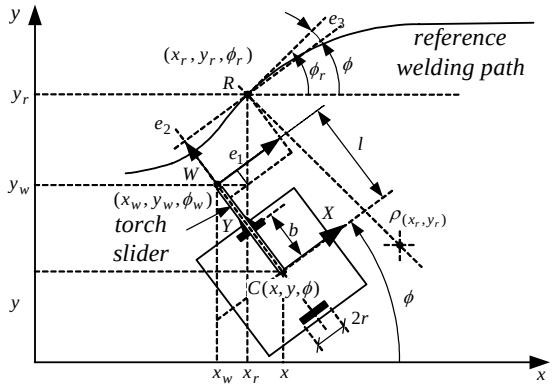

Fig. 2 Scheme for deriving WMR kinematic equations

The derivative of (7) yields

$$\begin{bmatrix} \dot{x}_w \\ \dot{y}_w \\ \dot{\phi}_w \end{bmatrix} = \begin{bmatrix} \cos\phi & -l\cos\phi \\ \sin\phi & -l\sin\phi \\ 0 & 1 \end{bmatrix} \begin{bmatrix} v \\ \omega \end{bmatrix} + \begin{bmatrix} -\dot{l}\sin\phi \\ \dot{l}\cos\phi \\ 0 \end{bmatrix} \tag{8}$$

It is assumed that a reference point $R(x_r, y_r)$ on the reference path moving at the constant velocity of $v_r > 0$ with the orientation angle ϕ_r for all t. It is also assumed that the reference angular velocity ω_r is the rate of angular change of v_r, bounded and have bounded derivative for all t. The dynamic equation is shown below

$$\begin{cases} \dot{x}_r = v_r\cos\phi_r \\ \dot{y}_r = v_r\sin\phi_r \\ \dot{\phi}_r = \omega_r \end{cases} \tag{9}$$

where ϕ_r is defined as the angle between v_r and x axis.

3. TRACKING CONTROLLER DESIGN

The scheme of errors are shown in Fig. 2, and the tracking errors $\mathbf{e} = [e_1, e_2, e_3]^T$ are defined as the following

$$\mathbf{e} = \begin{bmatrix} e_1 \\ e_2 \\ e_3 \end{bmatrix} = \begin{bmatrix} \cos\phi & \sin\phi & 0 \\ -\sin\phi & \cos\phi & 0 \\ 0 & 0 & 1 \end{bmatrix} \begin{bmatrix} x_r - x_w \\ y_r - y_w \\ \phi_r - \phi_w \end{bmatrix} \tag{10}$$

Since $\dot{l} = 0$ for the fixed torch, the first derivative of errors yields

$$\begin{bmatrix} \dot{e}_1 \\ \dot{e}_2 \\ \dot{e}_3 \end{bmatrix} = \begin{bmatrix} -1 & e_2 + l \\ 0 & -e_1 \\ 0 & -1 \end{bmatrix} \begin{bmatrix} v \\ \omega \end{bmatrix} + \begin{bmatrix} v_r\cos e_3 \\ v_r\sin e_3 \\ \omega_r \end{bmatrix} \tag{11}$$

Step 1: Kinematic Controller Design

A kinematic controller is designed to achieve $e_i \to 0$ when $t \to \infty$; in other words, the welding point W tracks to the reference point R at a desired welding velocity.

The Lyapunov function candidate is chosen as

$$V_1 = \frac{1}{2}(e_1^2 + e_2^2) + \frac{1}{k_2}(1 - \cos e_3) \tag{12}$$

The derivative of V_1 becomes

$$\dot{V}_1 = e_1\dot{e}_1 + e_2\dot{e}_2 + \frac{1}{k_2}\sin e_3\dot{e}_3$$

$$= e_1(-v_d + v_r\cos e_3) + \frac{1}{k_2}\sin e_3(\omega_r - \omega + k_2 e_2 v_r)$$

(13)

To achieve $\dot{V}_1 \le 0$, the control law called virtual control for the mobile platform is chosen as the following:

$$\begin{aligned} v &= v_d = v_r \cos e_3 + k_1 e_1 \\ \omega &= \omega_d = \omega_r + k_2 v_r e_2 + k_3 \sin e_3 \end{aligned} \tag{14}$$

where v_d and ω_d are considered as its desired virtual control variables.

Substituting (14) into (13) yields the following

$$\dot{V}_1 = -k_1 e_1^2 - \frac{k_3}{k_2} \sin^2 e_3 \le 0 \tag{15}$$

clearly, $\dot{V}_1 \le 0$ and the tracking errors $\mathbf{e} = [e_1, e_2, e_3]^T$ is bounded along the system's solution. It is also assumed that not only the velocity of $v_r > 0$ is constant with the orientation angle ϕ_r but also the reference angular velocity ω_r is bounded and have its bounded derivative for all t in case of the welding mobile robot used in this paper, using Eqs. (11) and (15), it is shown that $\|\mathbf{e}\|$ and $\|\dot{\mathbf{e}}\|$ are bounded, so that $\left\|\ddot{V}_1\right\| < \infty$, i.e., $\dot{V}_1$ is uniformly continuous. Since $V_1(t)$ does not increases and converges to some constant value, by Barbalat's lemma, $\dot{V}_1 \to 0$ as $t \to \infty$. As $t \to \infty$, the limit of Eq. (15) becomes

$$0 = K_1 K_4 e_1^2 + K_3 e_3^2 \tag{16}$$

Eq. (16) implies that $[e_1 \quad e_3]^T \to 0$ as $t \to \infty$.

From Eq. (22), the derivative of error e_3 is given:

$$\dot{e}_3 = \omega_r - \omega \tag{17}$$

Substituting ω in Eq. (17) by the auxiliary control input ω_d (Eq. (14)), the following is yielded:

$$\dot{e}_3 = -k_2 e_2 v_r - k_3 \sin e_3 \tag{18}$$

Since $e_3 \to 0$ as $t \to \infty$, the limit of Eq. (18) yields

$$\dot{e}_3 = -k_2 e_2 v_r \tag{19}$$

Since equation $v_r^2 e_3$ has the limit equal to zero when $t \to \infty$, the derivative of this equation yields

$$\frac{d}{dt}\left(v_r^2 e_3\right) = -k_2 v_r^3 e_2 \tag{20}$$

$v_r^3 e_2$ is uniformly continuous since its time derivative is bounded. From Barbalat's Lemma, $\frac{d}{dt}\left(v_r^2 e_3\right)$ tends to zero. Therefore, $v_r^3 e_2$ tends to zero, and thus $v_r e_2$ tends to zero. Because the velocity of v_r is constant, $e_2 \to 0$ as $t \to \infty$ from Eq. (20). Hence, the equilibrium point $\mathbf{e} = 0$ is uniformly asymptotically stable.

Step 2: Adaptive Control Design

v and ω are considered as virtual control variables for the mobile robot. The control objective is that the trajectory tracking error e converges to zero asymptotically and v, ω converge to v_d, ω_d, respectively even in the presence of unknown parameters in the model of the dynamic system. To solve the above problem, $\tilde{v}$ and $\tilde{\omega}$ are defined as virtual control errors:

$$\begin{aligned} \tilde{v} &= v - v_d \\ \tilde{\omega} &= \omega - \omega_d \end{aligned} \tag{21}$$

Total error vector is defined as

$$\boldsymbol{\varepsilon} = [e_1, e_2, e_3, \tilde{v}, \tilde{\omega}]^T \tag{22}$$

The time derivative of the virtual control error can be derived as follows:

$$\begin{aligned} \dot{\tilde{v}} &= \dot{v} - \dot{v}_d = b_1 u_1 - \dot{v}_d \\ \dot{\tilde{\omega}} &= \dot{\omega} - \dot{\omega}_d = b_2 u_2 - \dot{\omega}_d \end{aligned} \tag{23}$$

Proof.

From the nonholonomic constraint (3), the derivative of v is

$$\begin{aligned} \dot{v} &= \ddot{x}\cos\phi - \dot{x}\sin\phi\dot{\phi} + \ddot{y}\sin\phi + \dot{y}\cos\phi\dot{\phi} \\ &= \left(\frac{\lambda}{m}\sin\phi + b_1 u \cos\phi\right)\cos\phi - \dot{x}\sin\phi\dot{\phi} + \\ &\left(-\frac{\lambda}{m}\cos\phi + b_1 u_1 \sin\phi\right)\sin\phi + \dot{y}\cos\phi\dot{\phi} \\ &= \frac{\lambda}{m}\sin\phi\cos\phi + b_1 u \cos^2 u - \dot{x}\sin\phi\dot{\phi} \\ &-\frac{\lambda}{m}\cos\phi\sin\phi + b_1 u_1 \sin^2\phi + \dot{y}\cos\phi\dot{\phi} \\ &= b_1 u_1 - (\dot{x}\sin\phi - \dot{y}\cos\phi)\dot{\phi} = b_1 u_1 = \frac{1}{\beta_1} u_1 \end{aligned} \tag{24}$$

$$\dot{\omega} = b_2 u_2 = \frac{1}{\beta_2} u_2 \tag{25}$$

where $\beta_1 = 1/b_2 = rm \neq 0$ and $\beta_2 = 1/b_2 = \frac{rI}{b} \neq 0$. From Eqs. (13), (14) and (21), the derivative of V_1 is

$$\begin{aligned}\dot{V}_1 &= e_1(-v_d - \tilde{v} + v_r \cos e_3) \\ &\quad + \frac{1}{k_2}\sin e_3(\omega_r - \omega_d - \tilde{\omega} + k_2 e_2 v_r) \\ &= -k_1 e_1^2 - \frac{k_3}{k_2}\sin^2 e_3 - \tilde{v}e_1 - \tilde{\omega}\frac{1}{k_2}\sin e_3\end{aligned} \quad (26)$$

where k_1, k_2 and k_3 are positive constants.

To obtain the dynamic mobile platform control law, a nonlinear feedback control $u \in R^{n-m}$ must be designed so that $v \to v_d$ as $t \to \infty$. It cannot be guaranteed that Eq. (26) has always negative value due to $\tilde{v}$ and $\tilde{\omega}$.

Consider the new Lyapunov function candidate

$$V_2 = V_1 + \frac{1}{2}(\tilde{v}^2 + \tilde{\omega}^2) + \frac{|b_1|}{2\gamma_1}\tilde{\beta}_1^2 + \frac{|b_2|}{2\gamma_2}\tilde{\beta}_2^2 \quad (27)$$

where $\tilde{\beta}_1 = \beta_1 - \hat{\beta}_1 = \frac{1}{b_1} - \hat{\beta}_1$ and $\tilde{\beta}_2 = \beta_2 - \hat{\beta}_2 = \frac{1}{b_2} - \hat{\beta}_2$

The time derivative of V_2 is

$$\dot{V}_2 = \dot{V}_1 + \tilde{v}\dot{\tilde{v}} + \tilde{\omega}\dot{\tilde{\omega}} + \frac{|b_1|}{\gamma_1}\tilde{\beta}_1\dot{\tilde{\beta}}_1 + \frac{|b_2|}{\gamma_2}\tilde{\beta}_2\dot{\tilde{\beta}}_2 \quad (28)$$

$$\begin{aligned}&= -k_1 e_1^2 - \frac{k_3}{k_2}\sin^2 e_3 + \tilde{v}(-e_1 - \dot{v}_d + \frac{u_1}{\hat{\beta}_1}) \\ &+ \tilde{\omega}(-\frac{1}{k_2}\sin e_3 + \frac{u_2}{\hat{\beta}_2} - \dot{\omega}_d) + \frac{\tilde{\beta}_1|b_1|}{\gamma_1}(-\gamma_1 \tilde{v}\, sign(b_1)\frac{u_1}{\hat{\beta}_1} - \dot{\hat{\beta}}_1) \\ &+ \frac{\tilde{\beta}_2|b_2|}{\gamma_2}(-\gamma_2 \tilde{v}\, sign(b_2)\frac{u_2}{\hat{\beta}_2} - \dot{\hat{\beta}}_2)\end{aligned} \quad (29)$$

To achieve $\dot{V}_2 \leq 0$, the following adaptive control law is chosen as:

$$\begin{cases} u_1 = \hat{\beta}_1(-c_1\tilde{v} + e_1 + \dot{v}_d) \\ u_2 = \hat{\beta}_2(-c_2\tilde{\omega} + \frac{1}{k_2}\sin e_3 + \dot{\omega}_d) \\ \dot{\hat{\beta}}_1 = -\gamma_1 \tilde{v}\ sign(b_1)(-c_1\tilde{v} + e_1 + \dot{v}_d) \\ \dot{\hat{\beta}}_2 = -\gamma_2 \tilde{\omega}\ sign(b_2)(-c_2\tilde{\omega} + \frac{1}{k_2}\sin e_3 + \dot{\omega}_d) \end{cases} \quad (30)$$

where c_1, c_2, γ_1, and γ_2 are positive constant and $\hat{\beta}_1$ is an estimate of β_1 and $\hat{\beta}_2$ is an estimate of β_2.

Since V_2 is lower bounded and $\dot{V}_2$ is negative semi-definite, V_2 converges to a finite limit. Also, $V_2\ e_1, e_2, e_3, \tilde{v}, \tilde{\omega}, \hat{\beta}_1$, and $\hat{\beta}_2$ are all bounded.

$$\dot{V}_2 = -k_1 e_1^2 - \frac{k_3}{k_2}\sin^2 e_3 - c_1\tilde{v}^2 - c_2\tilde{\omega}^2 \leq 0 \quad (31)$$

Furthermore, the second derivative of V_2 can be written as

$$\begin{aligned}\ddot{V}_2 &= -2k_1 e_1[(e_2 + l)(\omega_r + k_2 v_r e_2 + k_3 \sin e_3 + \tilde{\omega}) \\ &- (v_r \cos e_3 + k_1 e_1 + \tilde{v}) + v_r \cos e_3] \\ &- 2\frac{k_3}{k_2}\sin e_3 \cos e_3[\omega_r - (\omega_r + k_2 v_r e_2 + k_3 \sin e_3) - \tilde{\omega})] \\ &- 2c_1\tilde{v}[b_1\hat{\beta}_1(-c_1\tilde{v} + e_1 + \dot{v}_d) - \dot{v}_d] \\ &- 2c_2\tilde{\omega}[b_2\hat{\beta}_2(-c_2\tilde{\omega} + \frac{1}{k_2}\sin e_3 + \dot{\omega}_d) - \dot{\omega}_d]\end{aligned} \quad (32)$$

With the assumption that v_r, ω_r and their derivatives are bounded and from the above results, $\ddot{V}_2$ is bounded, that is, $\dot{V}_2$ is uniformly continuous. Since $V_2(t)$ is differentiable and converges to some constant value and that $\ddot{V}_2$ is bounded, by Barbalat's lemma, $\dot{V}_2(t) \to 0$ as $t \to \infty$. This, in turn, implies that $e_1, e_3, \tilde{v}$, and $\tilde{\omega}$ converge to zero. Then $e_2 \to 0$ when $t \to \infty$ as the same way of kinematic controller. $\tilde{\beta}_1, \tilde{\beta}_2$ converge to constant values because $\hat{\beta}_1, \hat{\beta}_2$ converge to some constant values when $t \to \infty$ from (30) and β_1, β_2 are unknown constant values.

4. MEASUREMENT OF THE ERRORS

In this paper, the controller is derived from measurement of the tracking errors e_1, e_2, e_3. The errors measurement scheme is described in Fig. 3: the two rollers are placed at O_1 and O_2. The roller at O_1 is used to specify the two errors e_1 and e_2 and the other, error e_3. The distance between the two rollers O_1O_2 is chosen according to the curve radius of the reference welding path at the contact $R(x_r, y_r)$ such as $\vec{v}_r // \overrightarrow{O_1O_2}$. The rollers' diameter is chosen small enough to overcome the friction force.

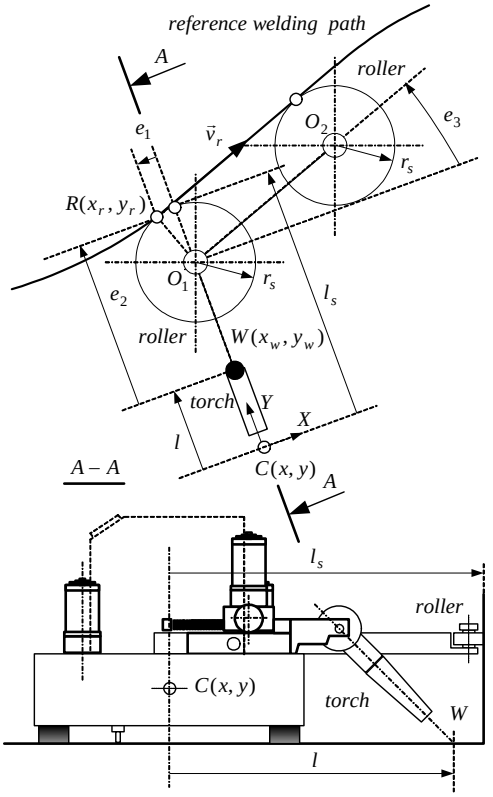

Fig. 3 Scheme for measuring the errors

From Fig. 3, the relationships are as follows:

$$\begin{cases} e_1 = -r_s \sin e_3 \\ e_2 = (l_s - l) - r_s(1 - \cos e_3) \\ e_3 = \angle(O_1C, O_1O_2) - \pi/2 \end{cases} \quad (33)$$

where r_s is the radius of roller, and l_s is the length of sensor. And the two potentiometers are used for measuring the errors: one linear potentiometer for measuring $(l_s - l)$ and one rotating potentiometer, the angular between X coordinate of WMR and $\vec{v}_r$.

5. THE EXPERIMENT DEVELOPMENT AND SIMULATION RESULTS

5.1 The experiment development

The control system was modularized on function to perform special control. The control system is based on the integration of three PIC18F452's: two for servo DC motor controllers, and one for main controller. The two servo controllers can perform indirect servo control using one encoder. The main controller which functions as master links to the two servo controllers, as slave, via I2C communication. The two A/D ports on master are connected to the two potentiometers for sensing the errors, as mentioned in section 4. The total configuration of the control system is shown in Fig. 4.

For operation, the main controller receives signals from sensors to achieve the errors, then the control laws are rendered based on the errors for the sampling time of 10ms, and send the results commands to the two servo controllers via I2C, respectively. The controller of the system is shown in Fig. 5.

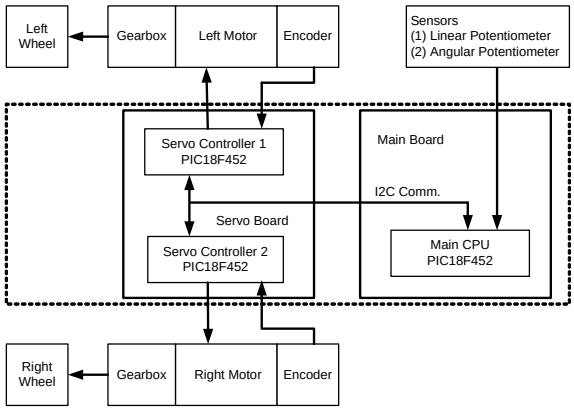

Fig. 4 The configuration of the control system

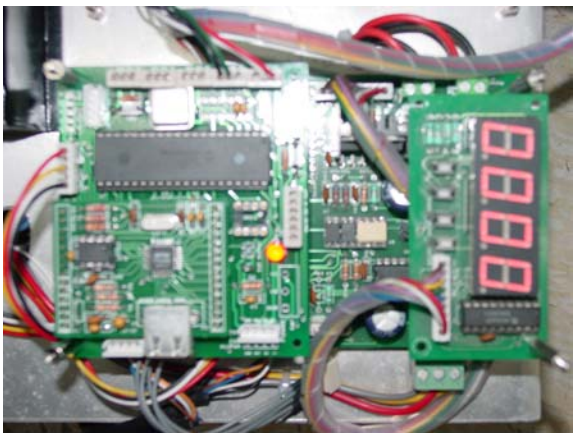

Fig. 5 The controller of the system

The experimental welding mobile robot is shown in Photo. 1.

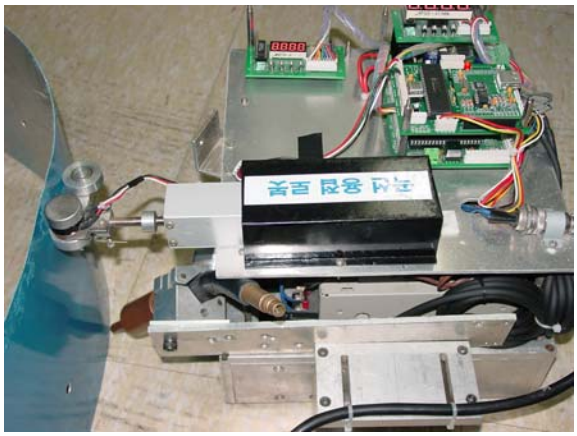

Photo. 1 The experimental welding mobile robot

5.2 The simulation results

To verify the effectiveness of the proposed controller, simulations have been done with adaptive controller (29) with a defined reference smooth curved welding path (Fig. 6).

Table 1. The initial values for the simulation

Parameters	Values	Unit
x_r	0.28	m
x_w	0.270	m
y_r	0.4	m
y_w	0.390	m
ϕ_{r}	20	deg.
ϕ_w	0	rad/s
v	0	m/s
ω	0	rad/s
l	0.24	m

The const parameters are chosen as $c_1 = c_2 = 100$, $\gamma_1 = \gamma_2 = 10$ and $b = 0.25m$. The robot's dynamic parameters are chosen as $b_1 = b_2 = 0.5$, which are assumed to be unknown but known signs. The WMR's initial values for the simulation are given in Table 1. The welding speed is 7.5 mm/s.

The simulation and experimental results are given through Figs. 7-19. In Fig. 7, it can be seen that the errors go to zeros after 5 seconds due to the motion of the fixed torch. Figs. 8-10 show nonfiltered data(a) and filtered data of tracking errors for experimental results. It is shown that the experimental data are bounded around simulation data. The filtered data is smoother than the nonfiltered data.

The two estimation values $\hat{\beta}_1$ and $\hat{\beta}_2$ are given in Figs. 11 and 12. The virtual linear velocity input v_d for kinematic controller and real linear velocity v for dynamic controller are shown in Fig. 13 for kinematic controller. The virtual angular velocity input ω_d for kinematic controller and real angular velocity ω for dynamic controller are shown in Fig. 14 for kinematic controller. The error of virtual velocity control error $\tilde{v}$ and $\tilde{\omega}$ approaches zero in Fig. 15 after 3 seconds. Fig. 16 show control inputs u_1 and u_2. Fig. 17 shows torques T_1 and T_2 of right and left wheels of MWR, respectively. Fig. 18 shows wheel velocities(rpm) of right and left wheels of MWR The posture and the welding trajectory are shown in Fig. 193.

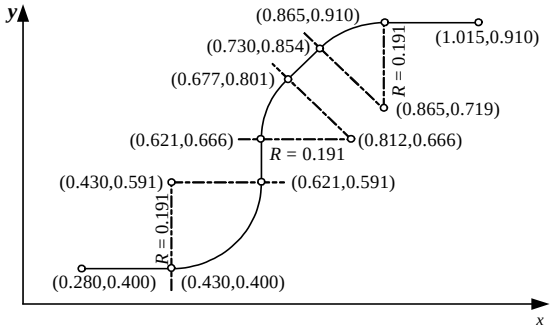

Fig. 6 Reference welding path

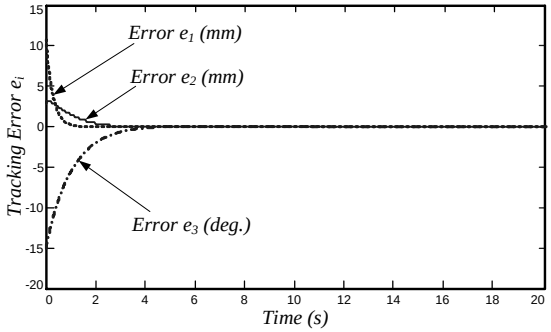

Fig.7 Tracking errors

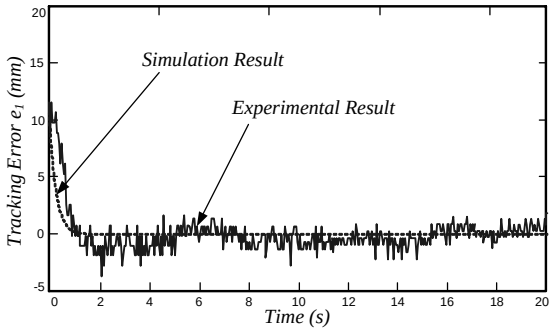

(a) nonfiltered data

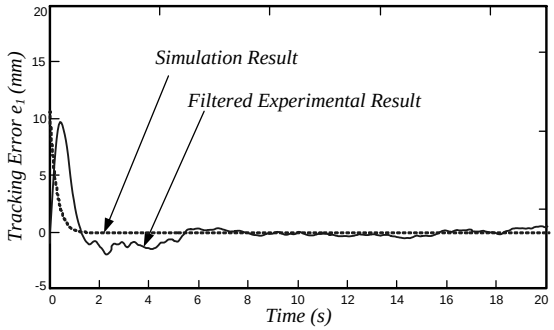

(b) filtered data

Fig.8 Tracking error e_1

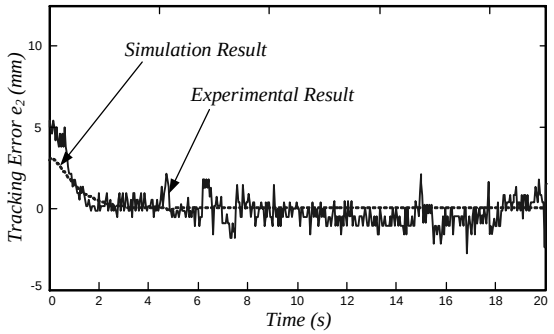

(a) nonfiltered data

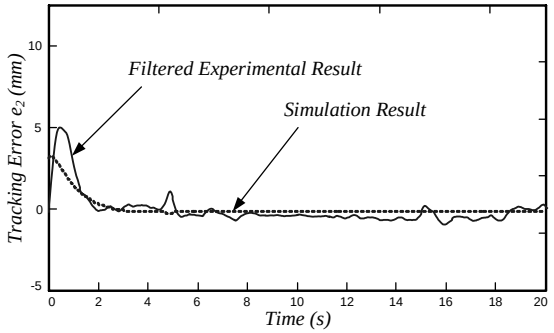

(b) filtered data

Fig. 9 Tracking error e_2

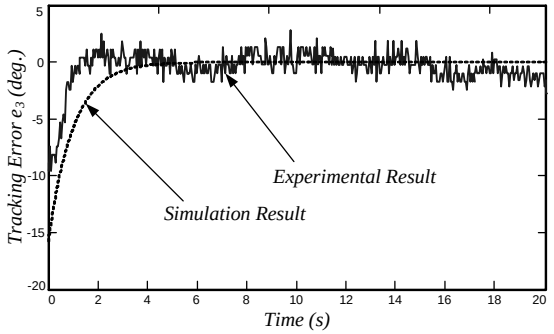

(a) nonfiltered data

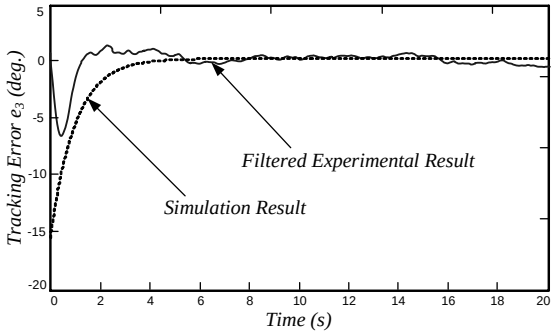

(b) filtered data

Fig. 10 Tracking error e_3

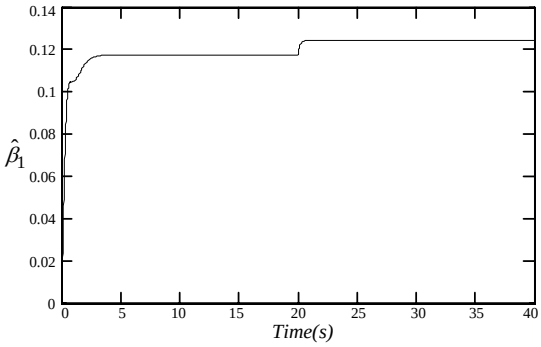

Fig. 11 Estimation of β_1

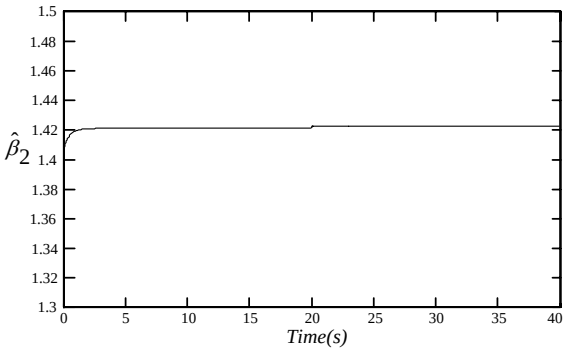

Fig. 12 Estimation of β_2

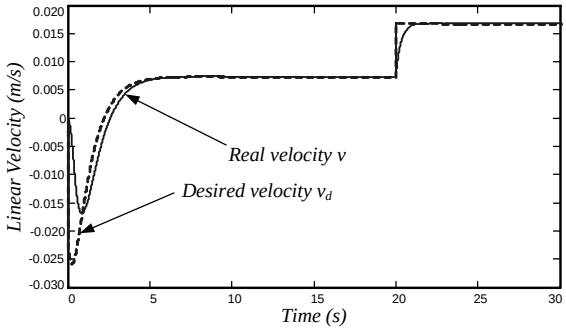

Fig. 13 Linear velocity of WMR

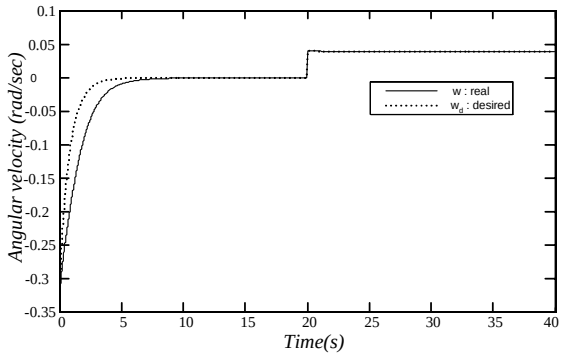

Fig. 14 Angular velocity of WMR

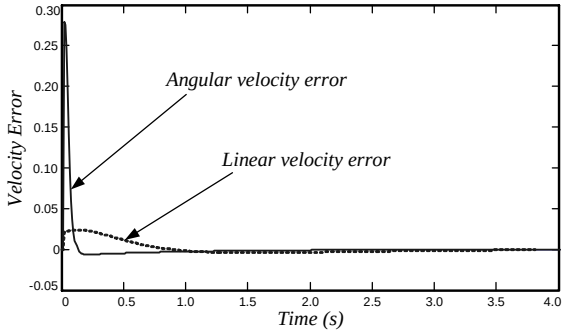

Fig. 15 Virtual velocity control errors

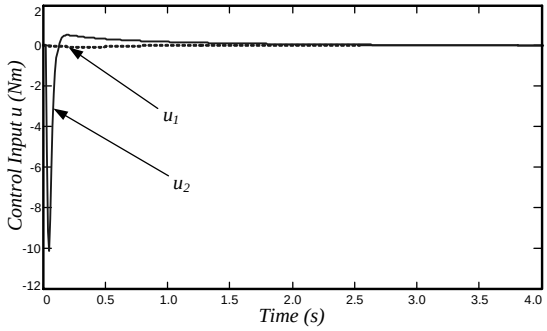

Fig. 16 Control inputs

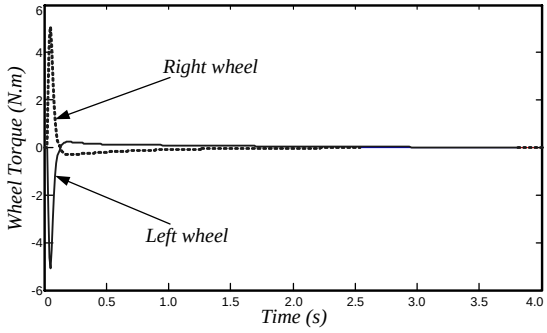

Fig. 17 Torque

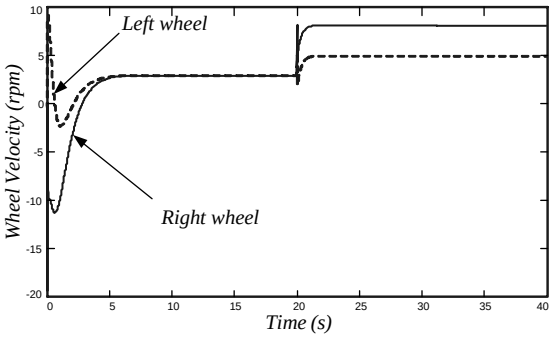

Fig. 18 Wheel velocity

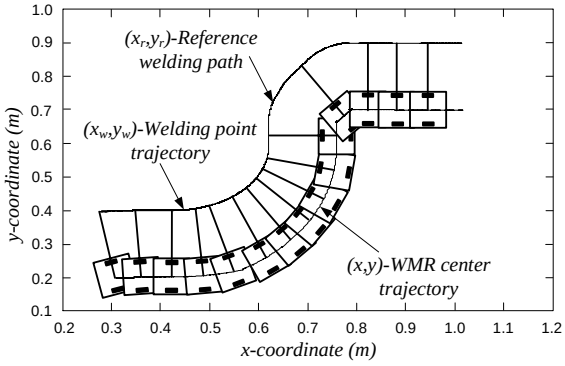

Fig. 19 WMR's movement tracking reference welding path

6. CONCLUSIONS

In this paper, an adaptive controller is proposed for welding mobile robot with unknown parameters such as mass, moment of inertia, wheel radius and length of the mobile platform to track smooth curved welding path. The controller is designed based on backstepping method using Lyapunov function. The mobile robot was considered in kinematic and dynamic models with unknown parameters of mass, moment of inertia, wheel radius and length of the mobile platform. To design the controller, an error configuration is defined. And then, a simple way of measuring the errors for deriving the control law using two potentiometers was proposed. The simulation experimental results show that the controller is possible and applicable in the practical welding mobile robot. This control system of the proposed controller is simpler than the that proposed by Bui. three PIC18F452's for this controller and four PIC16F877's for Bui's controller are needed because one PIC for controlling torch slider in this proposed control system is not needed.

REFERENCES

1. T. Fukao, H. Nakagawa and N. Adachi, "Adaptive Tracking Control of a Nonholonomic Mobile

Robot," IEEE Transactions on Robotics and Automation, Vol. 16, No. 5, pp. 609-615, 2000.
2. T. H. Bui, T. L. Chung, T. T. Nguyen, and Kim Sang Bong, "Adaptive Tracking Control of Two-Wheeled Welding Mobile Robot with Smooth-Curved Welding Path," KSME International Journal of Control, Automation, and Systems, Vol. 1, No. 1, pp. 35-42, 2003.
3. R. Fierro and F.L. Lewis, "Control of a Non-holonomic Mobile Robot: Backstepping Kinematics into Dynamics," Proceedings of the 38th Conference on Decision & Control, Phoenix Arizona USA, pp. 2094-2099, 2001.
4. Xiaoping Yun and Yoshio Yamamoto, "Internal Dynamics of a Wheeled Mobile Robot," Proceedings of the IEEE/RSJ International Conference on Intelligent Robots and Systems, pp. 1288-1294, 1993.
5. Ti-Chung Lee, Ching-Hung Lee, and Ching-Chen Teng, "Adaptive Tracking Control of Nonholonomic Mobile Robot by Computed Torque," Proc. of the 38th IEEE Conference on Decision and Control, pp. 1254-1259, 1999.
6. Y. Kanayama, Y. Kimura, F. Miyazaki and T. Noguchi, "A Stable Tracking Control Method for a Non-Holonomic Mobile Robot," Proc. of the IEEE/RSJ Int. Workshop on Intelligent Robots and Systems, pp. 1236-1241, 1991.
7. Jean Jacques E. Slotine and Weiping Li, Applied Nonlinear Control, Prentice-Hall, 1991.
8. Kolmanovsky I and McClamroch NH, "Developments in Nonholonomic Control Problem," IEEE Control System Magazine, pp. 20-36, 1995.